14th International Conference on Applications of Statistics and Probability in Civil Engineering, ICASP14
Dublin, Ireland, July 9-13, 2023

Reliability-based topology optimization for multi-material structures

Junho Chun
Assistant Professor, School of Architecture, Syracuse University, Syracuse, USA

ABSTRACT: In order to prevent unexpected failures and potential catastrophic damage in components or systems, uncertainties in loads and material properties are taken into account during optimization. This is achieved through the use of Reliability-Based Topology Optimization (RBTO), which combines reliability analysis with optimization to produce engineering solutions with a satisfactory level of reliability. Complex building structures are often comprised of multiple materials and require diverse performance characteristics. Using a single material may not be feasible in these cases. Multi-material RBTO offers a solution by allowing for the optimized spatial distribution of various materials to meet diverse design objectives. This paper presents an investigation into multi-material RBTO that takes into account uncertainties in loads and material properties, as well as the behavior and characteristics of different candidate materials. The optimization algorithm used in this approach relies on gradient calculations of objective and constraint functions to efficiently converge to optimal solutions. The proposed RBTO framework is evaluated on structural optimization problems, and the results show that it can improve performance while satisfying probabilistic constraints accurately, thus increasing the efficiency and effectiveness of optimal design identification

Structural optimization is a process aimed at finding the most effective structural design that meets specified design requirements such as displacement, stress, and buckling resistance (Haftka and Gurdal (1992)). Topology optimization (TO; Bendsøe and Sigmund (2004)), a mathematical technique, is used to determine the optimal distribution of material within a specified design space. This is achieved by formulating an objective and constraints based on the specific requirements of the problem. The applications of topology optimization extend across several fields including mechanical (Carbonari et al. (2007)), aerospace engineering (Krog et al. (2004)), and medicine (Sutradhar et al. (2010)). In the field of structural engineering, topology optimization is utilized to design lateral-load resisting systems Chun et al. (2016, 2019) and identify practical design solutions for industry use. In multi-material design, TO is used to find optimal solutions for selective material distribution to meet a design objective with constraints such as thermal insulation and structural stiffness, weight, compliant mechanism, negative Poisson's response of material, stress, and multi-phase relaxation. TO is used to study functionally graded materials to improve structural performances with gradual distributions of materials, and applied to multiple stress-constrained compliant mechanism problems (Banh et al. (2021)). To handle multi-materials in TO, the tailored design variable update scheme has been proposed to solve the static compliance minimization problems Sanders et al. (2018). Multi-resolution schemes Filipov et al. (2016) and Graphics Processing Units (GPU) (Herrero-Pérez and Martínez Castejón (2021)) based TO have been developed to reduce the computational cost for large-scale optimization problems.

Reliability-Based Topology Optimization (RBTO), as referred to in Kharmanda et al. (2004), is the process of incorporating probabilistic objectives and constraints into topology optimization. The performance of a structure is evaluated in a probabilistic manner due to the inherent uncertainties in structural loads and material properties.

Building structures are often composed of complex hierarchies made up of different materials. As a result, designing structures that require diverse performance can be achieved by considering the spatial distribution of mixed materials. This paper presents multi-material RBTO, taking into account the behavior and characteristics of candidate materials in the presence of uncertainty in loads and material properties, to arrive at an optimal design.

1. Topology optimization

An optimization problem of linearized elastic system under small deformations subjected to surface tractions $\boldsymbol{t}$ aims to find a displacement field $\boldsymbol{u} \in \mathcal{U}$ such that

$$a(\boldsymbol{u},\boldsymbol{v}) = \int_{\Omega} \mathbf{C}(\mathbf{x})\varepsilon(\boldsymbol{u}) : \varepsilon(\boldsymbol{v}) d\mathbf{x},\ l(\boldsymbol{v}) = \int_{\Gamma_t} \boldsymbol{t}\cdot\boldsymbol{v}\, ds$$
$$\mathcal{V} := \left\{\boldsymbol{v} \in H^1(\Omega) : \boldsymbol{v}|_{\Gamma_D} = 0\right\}$$
$$\mathcal{U} := \left\{\boldsymbol{u} \in H^1(\Omega) : \boldsymbol{v}|_{\Gamma_D} = \boldsymbol{g}\right\} \tag{1}$$

where Γ_D is the Dirichlet boundary, $\mathbf{C}$ is the material elasticity tensor which is a function of density function $\boldsymbol{\rho}(\mathbf{x}) \in [0,1]$, Ω is the design domain containing admissible shapes and its boundary $\boldsymbol{\delta}\Omega$ consists of displacement (Γ_D) and traction boundary conditions (Γ_t and Γ_{t0}) in Figure 1, $\varepsilon(\boldsymbol{u}) = 1/2(\nabla\boldsymbol{u} + \nabla\boldsymbol{u}^T)$ is the second order linearized strain tensor, and $\mathcal{V}$ is the space of admissible displacements. For simplicity, let $\boldsymbol{g} = 0$ and subsequently, $\mathcal{V} = \mathcal{U}$. The problem of minimizing compliance in TO involves finding the stiffest layout of the material under applied loads and boundary conditions and is stated as:

$$\inf_{\rho} J(\rho) = \int_{\Gamma_t} \boldsymbol{t}\cdot\boldsymbol{u}\, ds = \int_{\Omega} \mathbf{C}(\rho)\varepsilon(\boldsymbol{u}) : \varepsilon(\boldsymbol{u}) d\boldsymbol{x}$$
$$\text{s.t. } g(\rho) = \frac{1}{|\Omega|}\int_{\Omega} m_v(\rho) d\boldsymbol{x} - \overline{V}_f \leq 0 \tag{2}$$

where $\overline{V}_f$ is the prescribed maximum volume fraction and $|\Omega|$ is the volume of design domain Ωm, and m_v is the interpolation function for the volume constraint. The elasticity tensor $\mathbf{C}$ is expressed using the material interpolation function $m(\boldsymbol{\rho}(\mathbf{x}))$, Solid Isotropic Material with Penalization (SIMP) model (Zhou and Rozvany (1991)) as

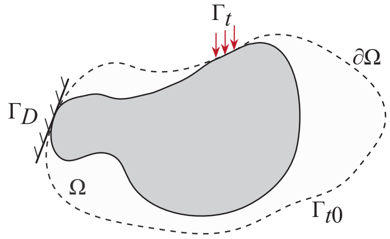

Figure 1: Illustration of the prescribed boundary conditions defined on the design domain Ω. The boundary $\partial\Omega$ consists of displacement boundary Γ_D, homogeneous Γ_{t0}, and non-homogeneous traction boundary Γ_t.

$$\mathbf{C}(\mathbf{x}) = m(\boldsymbol{\rho}(\mathbf{x}))\mathbf{C}^0$$
$$= \left[k_{min} + (1-k_{min})\boldsymbol{\rho}(\mathbf{x})^p\right]\mathbf{C}^0,\ k_{min} = 10^{-4} \tag{3}$$

where $\mathbf{C}^0$ denotes the elastic tensor of the solid element filled with material. To ensure the presence of solutions and enforce a minimum length scale in Eq. (2), the density fields are filtered using filtering schemes (Bendsøe and Sigmund (2004); Sigmund (2007)) such as

$$\hat{\rho}^e(\mathbf{x}) = \int_{\Omega} F(\mathbf{x},\mathbf{y})\rho(\mathbf{y}) d\mathbf{y} \tag{4}$$

where $\hat{\rho}^e(\mathbf{x})$ denotes the filtered density of element e and $F(\mathbf{x},\mathbf{y})$ is a kernel filter of radius R defined as:

$$F(\mathbf{x},\mathbf{y}) = c(\mathbf{x})\max\left(0, 1 - \frac{\mathbf{x}-\mathbf{y}}{R}\right)$$
$$c(\mathbf{x}) = \int_{\Omega} F(\mathbf{x},\mathbf{y}) d\mathbf{y} = 1 \tag{5}$$

1.1. Discretization

The solution to the optimal design problem in the continuous bilinear form can be approximated using the finite element method. The displacement field is discretized based on the finite element mesh. The Galerkin approximation to Eq. (1) can be stated as:

$$\mathbf{K}\mathbf{u} = \mathbf{f} \tag{6}$$

where $\mathbf{K}$, $\mathbf{u}$, and $\mathbf{f}$ are the stiffness matrix, nodal displacement vector and nodal force vector, respectively of a discretized elastostatics problem into finite elements. These can be expressed in the finite element

$$\begin{aligned}\mathbf{K}_{ij} &= \int_{\Omega} m(\boldsymbol{\rho}(\mathbf{x}))\mathbf{C}^0\nabla\mathbf{N}_i : \nabla\mathbf{N}_j d\mathbf{x} \\ &= \sum_{q=1}^{N_e} \int_{\Omega_q} m(\boldsymbol{\rho}(\mathbf{x}))\mathbf{C}^0\nabla\mathbf{N}_i : \nabla\mathbf{N}_j d\mathbf{x} \qquad (7) \\ \mathbf{f}_i &= \int_{\Gamma_t} \mathbf{t}\cdot\mathbf{N}_i ds\end{aligned}$$

where N_e is the number of elements and $\mathbf{N}_i$ is the basis for $\mathcal{V}_h(u_h \in \mathcal{V}_h; u_h(\mathbf{x}) = \sum_{m=1}^{N_{dof}} u_i N_i(\mathbf{x}))$. The linear filter in Eq. (5) in the finite element setting assigns a weighted average of the nearby densities of elements to each element. The filtered element density ρ^e at the centroid of element e ($\mathbf{x}^{e*}$) is computed by

$$\hat{\rho}^e = \rho(\mathbf{x}^{e*}) = \frac{\sum_{j\in\Omega} w_j^e \cdot \rho^j}{\sum_{j\in\Omega} w_j^e} \qquad (8)$$

and the linear weights w_j^e are obtained by

$$w_j^e = \max\left(\frac{R-r_j^e}{R}, 0\right) \qquad (9)$$

where R is the radius of linear filter that enforces a minimum member size, and r_j^e is the distance between centroids of elements e and j. The vector form of filtered elemental densities is written as

$$\hat{\rho} = \mathbf{P}\mathbf{z},\ \mathbf{P} = \left(w_j^e\right) \qquad (10)$$

where $\mathbf{z}$ is a set of design (density) variables.

2. Multi-material Topology optimization

TO for the multi-material, volume-constrained, compliance minimization problem (Sanders et al. (2018)) is stated

$$\begin{aligned}&\min_{\mathbf{z}_1,\cdots,\mathbf{z}_m} J = \mathbf{f}^T\mathbf{u}(\mathbf{z}_1,\cdots,\mathbf{z}_m) \\ &\text{s.t. } g_k = \sum_{i\in\eta_k}\sum_{e\in\chi_k} \hat{\rho}_i^e V^e - \overline{V}_k \le 0,\ k=1,\cdots,N_c \\ &\quad 0 \le \rho_i^e \le 1,\ i=1,\cdots,m,\ e=1,\cdots,N_e \\ &\text{with } \mathbf{K}(\mathbf{z}_1,\cdots,\mathbf{z}_m)\mathbf{u}(\mathbf{z}_1,\cdots,\mathbf{z}_m) = \mathbf{f}\end{aligned} \qquad (11)$$

where g_k are the volume constraints, $\mathbf{z}_1,\cdots,\mathbf{z}_m$ denote m density fields in the discretized design domain for each of the m materials, η_k is the set of material indices associated with constraint k, χ_k is the set of element indices associated with constraint j, $\hat{\rho}_i^e$ is the filtered density of material i in element e, V^e is the area (in the two-dimensional space; volume in three-dimensional space)) of element e, $\overline{V}_k$ is the prescribed maximum volume of constraint k, N_c is the number of constraints. Figure 2 shows a mesh with six triangular elements, three candidate materials, and three constraints. The set of material indices is defined as $\eta_1 = \{1,2,3\}, \eta_2 = \{1,3\}, \eta_3 = \{2\}$, and the set of element indices is $\chi_1 = \{\{4,5,6\},\{2,3\},\{1,2,3,4\}\}$, $\chi_2 = \{\{1,2,3\},\{5,6\}\}$, $\chi_3 = \{1,4,5,6\}$. The resulting set of design variables associated with η_k and χ_k is

$$\mathcal{D}_k = \{z_i^e | i \in \eta_k, e \in \chi_k\} \qquad (12)$$

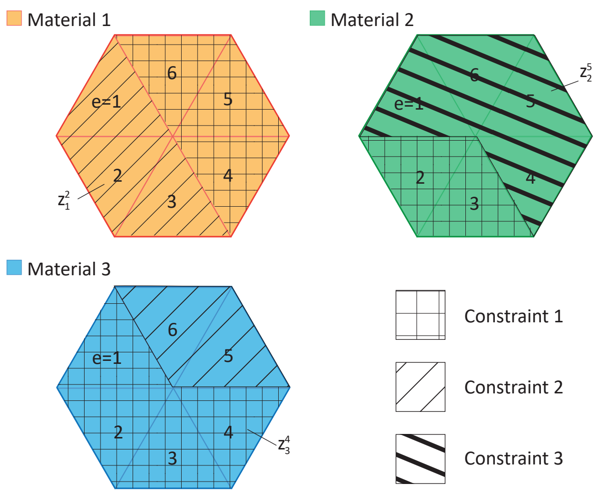

Figure 2: Illustration of the elements, materials, and constraints in multi-material TO. Design space is discretized with six elements and there are three candidate materials and three constraints.

In multi-material TO, the set of elasticity tensors of m materials at each elemental point is

$$\mathcal{S}(\mathbf{x}) = \{\mathbf{C}_1(\mathbf{x}),\cdots,\mathbf{C}_m(\mathbf{x})\} \qquad (13)$$

The elastic tensor $\mathbf{C}(\mathbf{x})$ is defined by choosing a finite set of m materials such as

$$\mathbf{C}(\mathbf{x}) = \mathcal{A}(\mathcal{S}(\mathbf{x})) \qquad (14)$$

Using Eq. (10), the filtered density of material i is obtained

$$\hat{\rho}_i(\mathbf{x}) = \mathbf{P}\mathbf{z}_i(\mathbf{x}), \;\; i = 1, \cdots, m \tag{15}$$

2.1. *Material interpolation*

For the elasticity tensor $\mathbf{C}(\mathbf{x})$ of m materials, a similar approach in the SIMP model is utilized to compute the penalized density for each material as

$$\bar{\rho}_i^e\,(\hat{\rho}_i^e) = (\hat{\rho}_i^e)^p \tag{16}$$

then the material interpolation function (Stegmann and Lund (2005)) is defined as

$$m^e(\bar{\boldsymbol{\rho}}^e(\mathbf{x})) = \sum_{i=1}^{m} \bar{\rho}_i^e \prod_{j=1, j\neq i} \left(1 - \bar{\rho}_j^e\right) E_i, \quad e = 1, \cdots, N_e \tag{17}$$

where E_i is the modulus of elasticity of material i.

3. Multi-material Reliability-based topology optimization

RBTO of the linearized elastic system problem with probabilistic constraints can be stated as ($\bar{\boldsymbol{\rho}} \equiv [\bar{\boldsymbol{\rho}}_1, \cdots, \bar{\boldsymbol{\rho}}_m]$):

$$\begin{aligned} &\min_{\mathbf{z}_1, \cdots, \mathbf{z}_m} f(\bar{\boldsymbol{\rho}}, \boldsymbol{\mu}_\psi) \\ &\quad \text{s.t. } P\left[g_i(\bar{\boldsymbol{\rho}}, \psi) \leq 0\right] \leq P^t, \; i = 1, ..., N_c \\ &\quad \text{with } \mathbf{K}(\bar{\boldsymbol{\rho}}, \psi)\mathbf{u}(\bar{\boldsymbol{\rho}}, \psi) = \mathbf{f}(\psi) \end{aligned} \tag{18}$$

g_i is the i-th limit-state function whose negative sign represents violation of a design constraint, $P[\cdot]$ is the probability of the violation of limit-state function, ψ is the vector of random variables, $\boldsymbol{\mu}_\psi$ is the vector of means of ψ, and P^t is the target failure probability. The probabilistic constraint in Eq. (18) can be formulated using the cumulative distribution function (CDF) of the limit state function such that

$$P\left[g_i \leq 0\right] = F_{g_i}(0) \leq \Phi(-\beta_i^t) \tag{19}$$

where $F_{g_i}(\cdot)$ denotes the CDF of the i-th limit-state function, $\Phi(\cdot)$ is the CDF of the standard normal distribution, and β_i^t is the target reliability index. The first-order/second-order reliability method (FORM/SORM (Der Kiureghian (2005)) can be used to evaluate the failure probability of the limit-state function. The nested optimization loops in Eq. 18 can be replaced with a single-loop approach (Liang et al. (2008)). A multi-material RBTO problem using a single-loop approach in the finite element setting is stated

$$\begin{aligned} &\min_{\mathbf{z}_1, \cdots, \mathbf{z}_m} f(\bar{\boldsymbol{\rho}}, \boldsymbol{\mu}_\psi) \\ &\quad \text{s.t. } g_{p_i} \cong g_i(\bar{\boldsymbol{\rho}}, \psi(\tilde{\mathbf{U}}_i^t)) \geq 0, \; i = 1, ..., N_c \\ &\quad \text{with } \mathbf{K}(\bar{\boldsymbol{\rho}}, \psi(\tilde{\mathbf{U}}_i^t))\mathbf{u}(\bar{\boldsymbol{\rho}}, \psi(\tilde{\mathbf{U}}_i^t)) = \mathbf{f}(\psi(\tilde{\mathbf{U}}_i^t)) \end{aligned} \tag{20}$$

where the approximated most probable failure point (MPP) of limit-state function i is computed as

$$\tilde{\mathbf{U}}_i^t \cong \beta_i^t \hat{\alpha}_i^t = \beta_i^t \left[-\frac{\nabla_\psi g_i(\bar{\boldsymbol{\rho}}, \psi(\mathbf{U}))\mathbf{J}_{\psi,\mathbf{U}}}{\left\| \nabla_\psi g_i(\bar{\boldsymbol{\rho}}, \psi(\mathbf{U}))\mathbf{J}_{\psi,\mathbf{U}} \right\|} \right]_{\mathbf{U}=\tilde{\mathbf{U}}_i} \tag{21}$$

where $\mathbf{U}$ is the vector of standard normal random variables, and $\mathbf{J}_{\psi,\mathbf{U}} (= \mathbf{J}_{\mathbf{U},\psi}^{-1})$ is the inverse of the Jacobian of the ψ to $\mathbf{U}$ transformation.

The i,j term of the stiffness matrix $\mathbf{K}$ in Eq. (7) in muti-material RBTO is rewritten as

$$\begin{aligned} \mathbf{K}_{ij} &= \int_\Omega m^e(\bar{\boldsymbol{\rho}}^e(\mathbf{x}), \mathcal{S}(\mathbf{x}), \psi)\mathbf{C}^0 \nabla \mathbf{N}_i : \nabla \mathbf{N}_j d\mathbf{x} \\ &= \sum_{e=1}^{N_e} \int_{\Omega_e} m^e(\bar{\boldsymbol{\rho}}^e(\mathbf{x}), \mathcal{S}(\mathbf{x}), \psi)\mathbf{C}^0 \nabla \mathbf{N}_i : \nabla \mathbf{N}_j d\mathbf{x} \end{aligned} \tag{22}$$

4. Sensitivity Analysis

A gradient-based optimization algorithm for solving the discrete problem in Eq. (20) requires the computation of the gradient of the objective and constraint functions. The derivative of compliance with respect to a design variable is

$$\frac{\partial J}{\partial z_i^e} = \frac{\partial J}{\partial m^e} \frac{\partial m^e}{\partial \bar{\rho}_j^k} \frac{\partial \bar{\rho}_j^k}{\partial \hat{\rho}_l^r} \frac{\partial \hat{\rho}_l^r}{\partial z_i^e}, \quad i = 1, \cdots, m, \;\; e = 1, \cdots, N_e \tag{23}$$

The sensitivity of compliance with respect to the material interpolation function can be derived as:

$$\frac{\partial J}{\partial m^e} = -\mathbf{u}^e(\mathbf{z}_1, \cdots, \mathbf{z}_m)^T \frac{\partial \mathbf{k}^e}{\partial m^e} \mathbf{u}^e(\mathbf{z}_1, \cdots, \mathbf{z}_m), \quad e = 1, \cdots, N_e \tag{24}$$

Note the derivative of the stiffness matrix of element e with respect to the material interpolation function is:

$$\begin{aligned}\frac{\partial \mathbf{k}^e}{\partial m^e} &= (1-k_{min})\mathbf{k}_0^e \\ \mathbf{k}_0^e &= \int_{\Omega_e} \mathbf{C}^0 \nabla \mathbf{N}_i : \nabla \mathbf{N}_j d\mathbf{x}\end{aligned} \tag{25}$$

The sensitivity of probabilistic compliance constraint $g(\bar{\boldsymbol{\rho}}, \boldsymbol{\psi})$ with respect to a random variable $\psi_k \in \boldsymbol{\psi}$ is obtained as:

$$\begin{aligned}\frac{\partial g(\bar{\boldsymbol{\rho}}, \boldsymbol{\psi})}{\partial \psi_k} =& 2\mathbf{u}(\bar{\boldsymbol{\rho}}, \boldsymbol{\psi})^T \frac{\partial \mathbf{f}(\boldsymbol{\psi})}{\partial \psi_k} \\ &- \mathbf{u}(\bar{\boldsymbol{\rho}}, \boldsymbol{\psi})^T \frac{\partial \mathbf{K}(\bar{\boldsymbol{\rho}}, \boldsymbol{\psi})}{\partial \psi_k} \mathbf{u}(\bar{\boldsymbol{\rho}}, \boldsymbol{\psi})\end{aligned} \tag{26}$$

Also, the sensitivity of the element stiffness matrix with respect to a random variable, modulus of elasticity of material k, $\psi_k = E_k$ can be computed by

$$\begin{aligned}\frac{\partial \mathbf{k}^e}{\partial E_k} &= (1-k_{min}) \frac{\partial m^e(\bar{\boldsymbol{\rho}}^e, \boldsymbol{\psi})}{\partial E_k} \mathbf{k}_0^e \\ &= \sum_{i=1}^{m} \bar{\rho}_i^e \prod_{j=1, j\neq i} \left(1-\bar{\rho}_j^e\right) \mathbf{k}_0^e, \\ e &= 1, \cdots, N_e\end{aligned} \tag{27}$$

Sensitivity of the limit state function with respect to a force random variable $\psi_k = f_k$ is derived as:

$$\frac{\partial g(\bar{\boldsymbol{\rho}}, \boldsymbol{\psi})}{\partial f_k} = 2\mathbf{u}(\bar{\boldsymbol{\rho}}, \boldsymbol{\psi})^T \frac{\partial \mathbf{f}(\boldsymbol{\psi})}{\partial f_k} = 2\mathbf{u}(\bar{\boldsymbol{\rho}}, \boldsymbol{\psi})^T \hat{\mathbf{f}} \tag{28}$$

where $\hat{\mathbf{f}}$ is a vector, whose j-th element is 1 if f_k is applied at the j-th degree of freedom, and 0 otherwise.

5. Numerical Examples

Two numerical examples demonstrate the feasibility of the present formulation for multi-material RBTO. Different combinations of random variables and statistical dependency are considered in multi-material RBTO, which will be stated for each numerical example. All materials are linear elastic and are defined by the modulus of elasticity E_k and Poisson's ratio ν_k for material k. Continuation on the SIMP penalty parameter, p is considered such that $p = 1$ is used at the start of the optimization process and is increased by 0.5 when every convergence criterion is met. The method of moving asymptotes (MMA; Svanberg (1987)) is used as an optimization algorithm with sensitivity in Section 4 to update design variables. The multi-material RBTO process is repeated until the convergence criteria on the maximum number of interactions or the relative change in the design variable is satisfied.

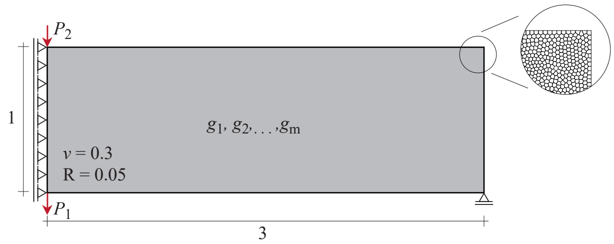

Figure 3: MBB beam design domain, loading and boundary conditions with constraints shown to control the entire domain.

5.1. MBB beam

The MBB beam subjected to point loads is considered to demonstrate the feasibility of the proposed method (Figure 3). The design domain is discretized with 5,000 polygonal elements. Material properties for five candidate materials with their associated volume constraints are in Figure 4. Magnitudes of applied forces (P_1, P_2) and modulus of elasticity E_k for material k are random variables which are assumed to follow the normal distribution. All random variables are statistically independent of each other, and the mean and coefficient of variation of random variables are summarized in Figure 5. An objective function is the minimization of failure probability of a compliance limit-state function defined as $P(\text{limit-state function} : J_{max}(=0.1) - J \leq 0)$ and a volume constraint for each of two, three, and four of the candidate materials is considered. The failure probability is estimated using the FORM.

The converged designs in Figure 6 show that the stiffest material is placed in areas in which the highest stresses are expected and less stiff material is distributed to the middle regions where stress is expected to be low. A lower failure probability of compliance limit-state function is obtained in a converged design with higher individual volume fractions of higher stiff materials.

Mat			1	2	3	4	5	Volume
E_k	$\times 10^5$		1.0	0.8	0.6	0.4	0.2	fraction
2-material	Fig. 6(a)	g_1	o	-	-	-	-	0.225
		g_2	-	o	-	-	-	0.225
3-material	Fig. 6(b)	g_1	o	-	-	-	-	0.15
		g_2	-	o	-	-	-	0.15
		g_3	-	-	-	-	o	0.15
4-material	Fig. 6(c)	g_1	-	o	-	-	-	0.1125
		g_2	-	-	o	-	-	0.1125
		g_3	-	-	-	o	-	0.1125
		g_4	-	-	-	-	o	0.1125

Figure 4: Candidate materials and specified volume constraints for 2, 3, and 4-material MBB beam.

Random variables	Marginal distribution	Mean	c.o.v	Correlation
Mat 1 E_1		1×10^5		
Mat 2 E_2		0.8×10^5		
Mat 3 E_3	Normal	0.6×10^5	0.2	Independent
Mat 4 E_4		0.4×10^5		
Mat 5 E_5		0.2×10^5		
P_1	Normal	2.5	0.1	Independent
P_2		3.0		

Figure 5: Description of random variables of applied forces and candidate materials for the MBB optimization design.

5.2. *Serpentine beam*

This numerical example is to demonstrate the capability of the present formulation to find optimal layouts of multi-materials while satisfying the probabilistic constraint. Five candidate materials for the serpentine beam design domain shown with boundary conditions in Figure 7 are considered in the example. The objective function is the minimization of the total volume of multi-materials. Each material is added to the objective function with the scale factor such as $\delta_i = 1/E_i \cdot \gamma$. The limit-state function for the probabilistic constraint is defined as $g : J_{max}(=0.1) - J \leq 0)$. The modulus of elasticity for material i and forces are random variables. Marginal distribution, mean, coefficient of variation and correlation coefficients are shown in

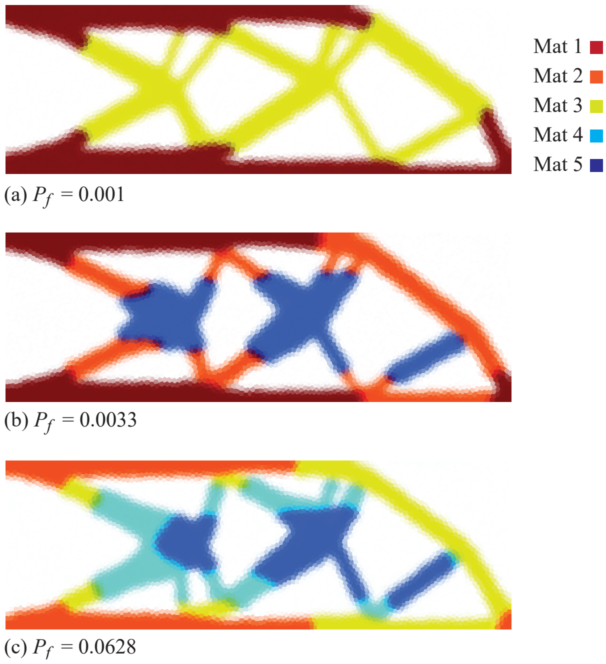

Figure 6: Multi-material MBB beam designs with individual volume constraints for each of (a) 2; (b) 3; and (c) 4 candidate materials. Failure probabilities (P_f) are based on the converged results.

Figure 8. The target failure probability of the constraint P_f is 0.001.

Figure 9 shows the results of RBTO considering a single probabilistic constraint with varying γ. It is noted that a higher γ in a scale factor applied to each material results in a converged design that is closer to a global optimum. Figure 10 shows the convergence history obtained using the present formulation for Figure 9(c). The proposed method can efficiently find a design solution that satisfies the probabilistic constraint within 20 iterations and keep reducing the volume fraction of each material until the convergence criteria are met. The volume fraction of each material for the converged design is summarized in Figure 11.

6. CONCLUSIONS

In this paper, a Multi-Material RBTO formulation is presented that is capable of considering an arbitrary number of materials with varying properties, probabilistic constraints, and differing marginal distributions. The sensitivities of compliance, probabilistic constraints with respect to design variables, material interpolation functions

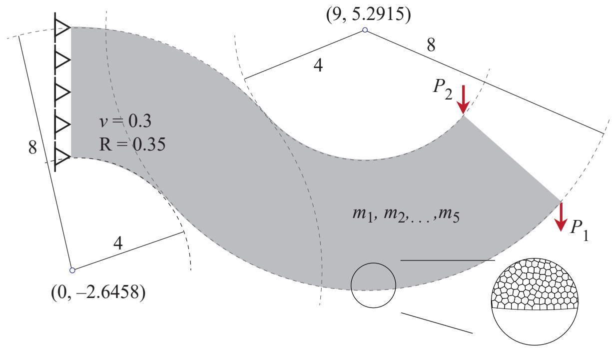

Figure 7: Serpentine design domain, loading and boundary conditions. The design space is discretized with 5,000 polygonal elements.

Random variables	Marginal distribution	Mean	c.o.v	Correlation
Mat 1 E_1	Normal	1×10^5	0.1	$\rho_{\text{Mat }i,\text{Mat }j} = 0.25$, $i \neq j$
Mat 2 E_2		0.8×10^5		
Mat 3 E_3		0.6×10^5		
Mat 4 E_4		0.4×10^5		
Mat 5 E_5		0.2×10^5		
P_1	Log-Normal	1.0	0.1	$\rho_{P_1,P_2} = 0.5$
P_2		1.5		

Figure 8: Description of random variables of applied forces and candidate materials for the serpentine beam design.

with multi-materials, and random variables are analytically derived. This opens up avenues for future research in the area of multi-material system reliability-based topology optimization. The multi-material RBTO framework for structures under dynamic and stochastic loads can be an avenue toward practical applications in practice.

ACKNOWLEDGEMENT

The author acknowledges the support of the Innovative and Interdisciplinary Research Program of Syracuse University (Grant no.II-50-2021).

7. REFERENCES

Banh, T. T., Luu, N. G., and Lee, D. (2021). "A non-homogeneous multi-material topology optimization approach for functionally graded structures with cracks." *Composite Structures*, 273, 114230.

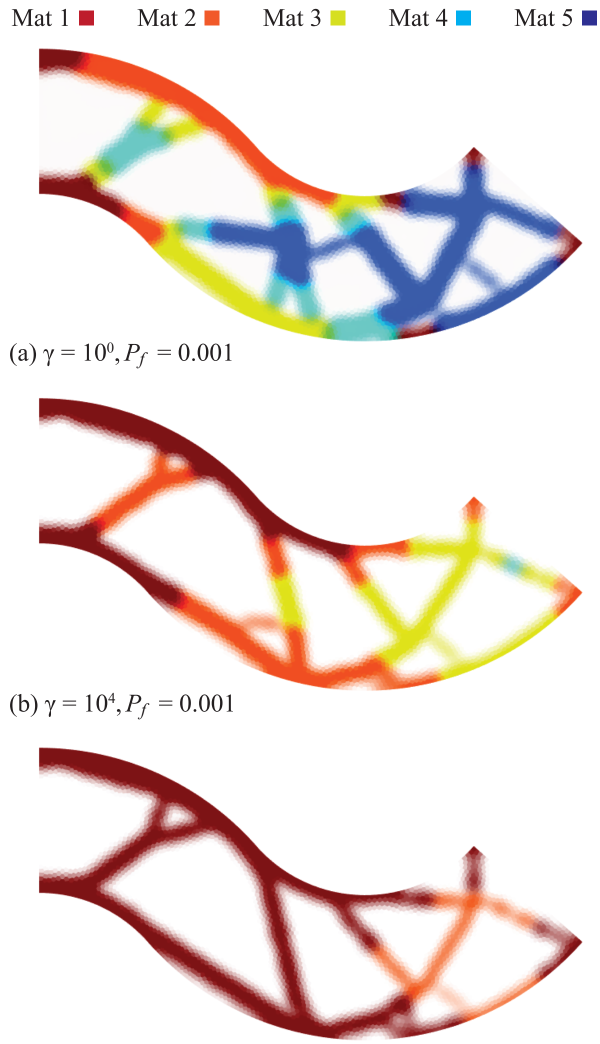

(a) $\gamma = 10^0, P_f = 0.001$

(b) $\gamma = 10^4, P_f = 0.001$

(c) $\gamma = 10^5, P_f = 0.001$

Figure 9: Multi-material serpentine beam designs satisfying the probabilistic constraint ($P_t = 0.001$) with varying γ. Failure probabilities (P_f) are based on the converged results.

Bendsøe, M. and Sigmund, O. (2004). *Topology optimization. Theory, methods, and applications. 2nd ed.*

Carbonari, R. C., Silva, E. C., and Paulino, G. H. (2007). "Topology optimization design of functionally graded bimorph-type piezoelectric actuators." *Smart Materials and Structures*, 16(6), 2605–2620.

Chun, J., Song, J., and Paulino, G. (2016). "Structural topology optimization under constraints on instantaneous failure probability." *Structural and Multidisciplinary Optimization*, 53(4).

Chun, J., Song, J., and Paulino, G. H. (2019). "System-reliability-based design and topology optimization of

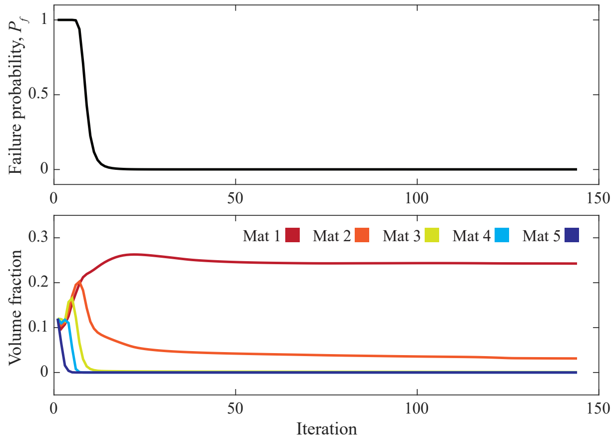

Figure 10: Convergence history of failure probability and volume fractions of candidate materials for Figure 9(c).

Material m	Fig.9(a)	Fig.9(b)	Fig.9(c)
Mat 1	0.0531	0.1104	0.2424
Mat 2	0.0814	0.1091	0.0310
Mat 3	0.0739	0.0746	0.0000
Mat 4	0.0646	0.0018	0.0000
Mat 5	0.1544	0.0000	0.0000
Total Volume	0.4274	0.3017	0.2747

Figure 11: Volume fraction of each material for the converged design shown in Figure9.

structures under constraints on first-passage probability." *Structural Safety*, 76, 81–94.

Der Kiureghian, A. (2005). "First- and Second-Order Reliability Methods." *Engineering Design Reliability Handbook*, CRC Press, Boca RatoN, Chapter 14.

Filipov, E. T., Chun, J., Paulino, G. H., and Song, J. (2016). "Polygonal multiresolution topology optimization (PolyMTOP) for structural dynamics." *Structural and Multidisciplinary Optimization*, 53(4), 673–694.

Haftka, R. T. and Gurdal, Z. (1992). *Elements of Structural Optimization: Third Edition*. Springer Netherlands.

Herrero-Pérez, D. and Martínez Castejón, P. J. (2021). "Multi-GPU acceleration of large-scale density-based topology optimization." *Advances in Engineering Software*, 157-158, 103006.

Kharmanda, G., Olhoff, N., Mohamed, A., and Lemaire, M. (2004). "Reliability-based topology optimization." *Structural and Multidisciplinary Optimization*, 26(5), 295–307.

Krog, L., Tucked, A., Kemp, M., and Boyd, R. (2004). "Topology optimization of aircraft wing box ribs." *Collection of Technical Papers - 10th AIAA/ISSMO Multidisciplinary Analysis and Optimization Conference*, Vol. 3, 2020–2030.

Liang, J., Mourelatos, Z., and Tu, J. (2008). "A single-loop method for reliability-based design optimization." *International Journal of Product Development - Int J Prod Dev*, 5.

Sanders, E. D., Aguiló, M. A., and Paulino, G. H. (2018). "Multi-material continuum topology optimization with arbitrary volume and mass constraints." *Computer Methods in Applied Mechanics and Engineering*, 340, 798–823.

Sigmund, O. (2007). "Morphology-based black and white filters for topology optimization." *Structural and Multidisciplinary Optimization*, 33, 401–424.

Stegmann, J. and Lund, E. (2005). "Discrete material optimization of general composite shell structures." *International Journal for Numerical Methods in Engineering*, 62, 2009 – 2027.

Sutradhar, A., Paulino, G. H., Miller, M. J., and Nguyen, T. H. (2010). "Topological optimization for designing patient-specific large craniofacial segmental bone replacements." *Proceedings of the National Academy of Sciences of the United States of America*, 107(30), 13222–13227.

Svanberg, K. (1987). "The method of moving asymptotes: a new method for structural optimization." *International Journal for Numerical Methods in Engineering*, 24(2), 359–373.

Zhou, M. and Rozvany, G. (1991). "The coc algorithm, part ii: Topological, geometrical and generalized shape optimization." *Computer Methods in Applied Mechanics and Engineering*, 89(1), 309–336 Second World Congress on Computational Mechanics.